Sensitivity Comparison of Macro- and Micro-Electrochemical Biosensors for Human Chorionic Gonadotropin (hCG) Biomarker Detection

SAMAR DAMIATI[1], **CARRIE HASLAM**[2], **SINDRE SØPSTAD**[3,4], **MARTIN PEACOCK**[3], **TOBY WHITLEY**[2], **PAUL DAVEY**[2], **AND SHAKIL A. AWAN**[2]

[1]Department of Biochemistry, Faculty of Science, King Abdulaziz University, Jeddah 21589, Saudi Arabia
[2]Wolfson Nanomaterials and Devices Laboratory, Faculty of Science and Engineering, School of Computing, Electronics and Mathematics, University of Plymouth, Plymouth PL4 8AA, U.K.
[3]Zimmer and Peacock Ltd., Royston SG8 9JL, U.K.
[4]Department of Microsystems, Faculty of Maritime and Natural Sciences, University of South-Eastern Norway, 3184 Borre, Norway

Corresponding author: Samar Damiati (samar.damiati@gmx.us)

ABSTRACT Selectivity and sensitivity are important figures of merit in the design and optimization of electrochemical biosensors. The efficiency of a fabricated immunosensing surface can easily be influenced by several factors, such as the detection limit, non-specific binding, and type of sensing platform. Here, we demonstrate the effects of macro- and micro-sized planner working electrodes (4 mm and 400 μm diameter, respectively) on electrochemical behavior and the ability of the developed biosensor to detect human chorionic gonadotropin (hCG), which is a biomarker of several tumors. The fabricated screen-printed sensor was constructed by modifying the carbon macro- and micro-electrodes with a linker, 1-pyrenebutyric acid-N-hydroxy-succinimide ester (PANHS), and immobilization of anti-hCG antibodies to specifically detect the hCG protein. The characterization of the developed electrodes was performed by cyclic voltammetry (CV) and square wave voltammetry (SWV). Each immunosensing system showed unique electrochemical behavior, which might be attributed to the arrangement of particles on the surface. However, a smaller micro-electrode surface area was found to show higher sensitivity (1 pg/mL) compared to the macro-electrode sensor with a lower detection limit of 100 pg/mL. Further, Raman spectroscopy analysis confirmed that the micro-electrode had a relatively low density of defects and disorder compared to the macro-electrode. The proposed assay represents a promising approach that is highly effective for specific detection of an analyte and can be exploited to target biomarkers for a variety of point-of-care diagnostic applications.

INDEX TERMS Macro-electrodes, micro-electrodes, electrochemical biosensors, screen printed carbon electrode (SPCE), human chorionic gonadotropin (hCG), tumor biomarker, diagnostics.

I. INTRODUCTION

The development of selective and sensitive immunosensors to quantify a small concentration of analytes is still a challenging task due to the difficulty of controlling the fabricated sensing surface. Several factors may impact the efficiency of the developed biosensor including the wettability properties of the sensing layer, the orientation and density of the captured biomolecules (antibodies or aptamers), and the choice of sensing platform, which must be inert to avoid any overlapping features of other materials on the surface of the sensing electrode [1]–[3]. Electrochemical analysis is one of the most widely used techniques in clinical applications due to its speed, low cost, design flexibility, and high sensitivity and selectivity [4]–[7]. Moreover, electrochemical-based biosensors can be exploited either to understand the

The associate editor coordinating the review of this manuscript and approving it for publication was Sanket Goel.

electrochemical behavior of biomolecules or as effective tools to detect different analytes in clinical, environmental, agricultural, pharmaceutical, and food samples [8]–[10]. Depending on the application, several features need to be considered in the functionalized electrode such as size, shape, structure, composition, morphology, and the material of the working electrode. An important parameter in developing an efficient sensor is the size of the most common planar working electrode. The performance of electrochemical measurements at the micron or submicron scale offers many advantages including (i) lower ohmic losses; (ii) reduced electrode capacitance due to the smaller surface area; (iii) an enhanced signal-to-noise ratio; (iv) changes in electrode surface diffusion from linear to radial, which increases the mass transport rates to and from the electrode; (v) reduced polarization time, which ultimately lowers the setup time and shortens the overall assay time and finally, (vi) permits electrochemical analysis of in vivo processes [11]–[13]. However, despite these advantages, micro-electrodes suffer from some limitations compared to macro-electrodes, such as the additional effort needed for cleaning and pretreatment (electrochemically and mechanically) to regenerate the electrode surface, the easy deactivation of matrix materials and chemical reactions with aggressive and organic solvents, and the requirement of a sensitive current amplifier for measuring currents in the micro-ampere range [14], [15]. They are often manufactured at the performance limits of the manufacturing process, and hence suffer from higher variability in the relative electrode area compared to macro-electrodes, which directly affects their sensitivity.

Generally, when it is difficult to obtain quantitative or qualitative voltammetric responses for the target analytes, an electro-catalytic mediator, such as a polymer or linker, can be used to modify the electrode surface to enhance the sensing performance of the fabricated sensor. There are several methods to immobilize mediator molecules onto the sensor including physical attachments, drop casting, physical or chemical covalent bond sorption, and mixing into the carbon paste [16]. 1-pyrenebutyric acid-N-hydroxy-succinimide ester (PANHS) is a linker that can be used as a scaffolding molecule to modify the electrode surface by providing a suitable base for immobilizing antibodies. PANHS has been immobilized on carbon or graphene sheets [17], [18] and carbon nanotubes through π-stacking, and its succinimidyl ester group can react strongly to nucleophilic substitution by the amine groups of an antibody or protein [19]–[21].

Human chorionic gonadotropin (hCG) is a 37 kDa glycoprotein hormone composed of two non-identical subunits: α-hCG (14 kDa, 92 amino acids), which can be found in different glycoprotein hormones, such as thyroid stimulating hormone, and β-hCG (23 kDa, 145 amino acids), which is unique to hCG. These two subunits are joined together by hydrophobic and ionic non-covalent interactions. This hormone is an important diagnostic marker of pregnancy and early fetal loss [22]–[24]. However, β-hCG is not found in healthy men, but the presence of the free β-subunit in blood is widely used as a tumor biomarker in selected tumors such as lung [25], stomach [26], and pancreas [27] tumors. Indeed, it has been recommended to combine blood and urine assays of β-hCG for the detection of cervical and ovarian cancers [28]. However, hCG is expressed by both trophoblastic and non-trophoblastic human malignancies and plays a critical role in cell growth, invasion, and malignancy at an advanced stage of cancer [29].

Carful optimization and functionalization of the sensors surface is an important approach. Many electrochemical biosensors have been developed to detect hCG by exploiting various biomaterials and metals to functionalize the sensor surface in order to improve the sensor sensitivity by amplifying the electrochemical signal. For example, nanomaterials (e.g., gold [30], platinum [31], and graphene [32]), polymers such as chitosan [32], and titania sol–gel film [33] are used to functionalize the working electrode and detect hCG electrochemically. A simple sensor architecture reduces the preparation time but still retains favorable selectivity and sensitivity for biosensor development. Label-free biosensors exhibit a simple measurement strategy that provides many advantages that overcome some limitations associated with the labeled systems. They are cheaper and faster due to requiring fewer materials and steps to develop the biosensing system. In this contribution, we report the effect of the working electrode diameter on the sensitivity detection of hCG via a label-free electrochemical-based biosensor at the picogram level. The designed biosensor is very simple. It is based on the functionalization of the carbon graphite electrode with a scaffolding molecule, PANHS, and an anti-hCG antibody. As shown in Scheme 1, the approach uses commercially available macro- and micro-sized working electrodes (4 mm and 400 μm in diameter, respectively). By optimizing the detection conditions and assessing the obtained signals from cyclic voltammetry (CV) and square wave voltammetry (SWV) measurements, efficient biosensors are developed. The fabricated micro-electrode exhibits a detection limit of 1 pg/mL compared to the macro-electrode with a ~100 pg/mL limit of detection (LoD). The performance of the micro-electrode exceeds several developed biosensors with more molecular decoration on the electrode surface.

II. EXPERIMENTAL SECTION

A. REAGENTS
The hCG antigen and antibody were purchased from Abcam, UK. Insulin, phosphate-buffered saline (PBS) tablets, bovine serum albumin (BSA), $K_3[Fe(CN)_6]$, $K_4[Fe(CN)_6]$, and KCl, were obtained from Sigma-Aldrich GmbH, Germany. Screen printed carbon macro- and micro-electrodes (SPCE) were obtained from DropSens (Spain) and Zimmer and Peacock (UK), respectively.

B. RAMAN SPECTROSCOPY
Raman spectra were collected using an XploRA Raman system (Horiba, Middlesex, UK) running LabSpec 6 and
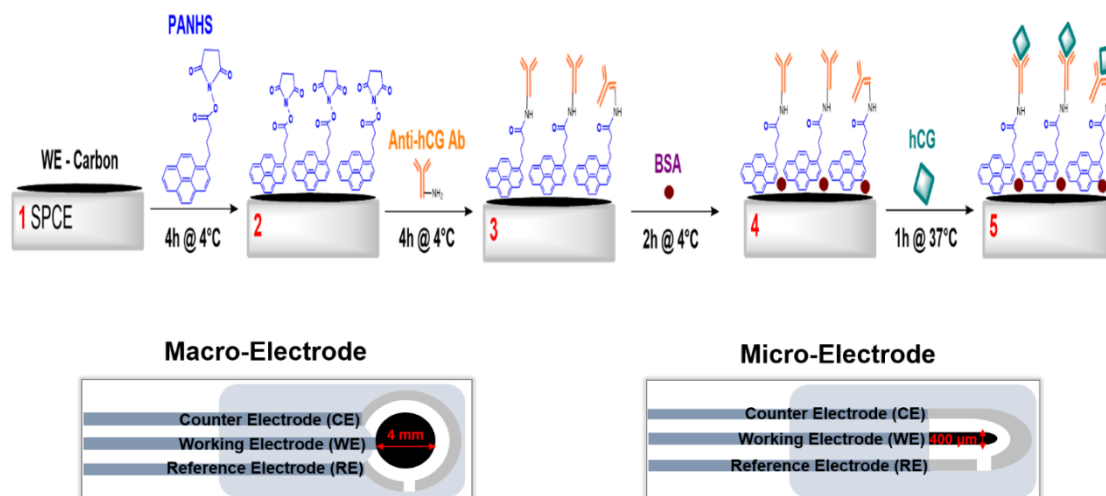
Scheme 1. Approach for the detection of hCG biomarker by modified macro- and micro-electrodes. Schematic showing the steps involved for the fabrication of electrochemical biosensor (not to scale) (1) bare screen printed carbon electrode (SPCE) either macro- or micro-electrode; (2) modification of electrode surface with PANHS; (3) immobilization of anti-hCG antibody; (4) blocking with BSA to prevent non-specific binding; (5) capturing of hCG antigen onto the modified surface and formation of antibody-antigen complex.

equipped with a 532 nm HeNe laser delivering ∼4mW of laser power at the sample. An Olympus BX41 microscope (Tokyo, Japan) with a 100 μm slit width and a 300 μm confocal hole, with 1200/mm gratings and 1000x magnification (resolution ∼0.26 μm). An MPlan N 100x microscope objective (NA of 0.90 and working distance 0.21 mm) focused the laser on the sample with a spot size of ∼7.5 μm diameter. A 1024 × 256 thermoelectrically cooled charge coupled device (CCD) camera was used for acquisition of Raman spectra at up to 1.48 MHz readout speed.

C. CONTACT ANGLES MEASUREMENTS
The contact angles of water on both the micro- and macro-electrodes of the sensor surface were measured using a goniometer (Easy Drop, Krüss, Germany). Briefly, 3–5 μL of Milli-Q water was deposited onto the sensor surface, and the angle was measured immediately at room temperature. All contact angle measurements were repeated at least in triplicate.

D. PREPARATION OF THE MODIFIED SENSOR
A three-electrode system consisting of a counter electrode (CE, carbon), reference electrode (RE, Ag for macro-electrode and Ag/AgCl for micro-electrode), and working electrode (WE, diameter of carbon macro- and micro-electrodes = 4 mm and 400 μm, respectively) was used in this study to perform the electrochemical measurements. Initially, working electrodes were incubated with 2 mM PANHS in methanol for 4 hours at 4 °C in a wet chamber. After rinsing with PBS, 20 μg/mL of anti-hCG antibodies was dropped on the surface and incubated for another 4 hours at 4 °C, followed by blocking with 0.5% BSA in PBS for at least 2 hours at 4 °C to minimize unspecific adsorption on the surface. A rinsing step with PBS was performed after each

step. The developed sensors were stored at 4 °C until further use. Different concentrations (from 1 pg/mL to 100 ng/mL) of hCG antigen in PBS were incubated with the modified electrodes for 60 min at 37 °C to form an antigen-antibody complex.

E. ELECTROCHEMICAL MEASUREMENTS
The sensor performance was investigated using cyclic voltammetry (CV) and square wave voltammetry (SWV). Cyclic voltammograms were recorded from −0.4 to 0.6 V for macro-electrodes and from −0.2 to 0.5 V for micro-electrodes at scan rates of 10 and 50 mV/s. Square wave voltammograms were recorded in the potential interval of 0.45 to −0.15 V under the following conditions: amplitude of 25 mV, frequency of 15 Hz, and an increase in potential of 5 mV, yielding an effective scan rate of 75 mV s^{-1}. All electrochemical measurements were performed in a solution of 10 mM [Fe(CN$_6$)]$^{3-}$ and 10 mM [Fe(CN$_6$)]$^{4-}$ (1:1), containing 100 mM KCl.

III. RESULTS AND DISCUSSION
A. CHARACTERIZATION OF BARE CARBON MACRO- AND MICRO-ELECTRODES BY RAMAN SPECTROSCOPY
Raman spectroscopy is a highly sensitive technique that enables characterization of the molecular morphology of carbon materials and provides information about their structure and properties. Previous studies have investigated the Raman spectra for before and after modification of SPE electrodes [34], [35]. In this study, Raman spectroscopy was used to analyze the carbon matrix of macro- and micro-electrodes. Figure 1 displays the Raman spectra from the macro- and micro-electrode surfaces. Raman peaks were observed at ∼1350, ∼1580 cm^{-1} and ∼2750 cm^{-1} which correspond to the disordered (D) band and graphitic (G) and
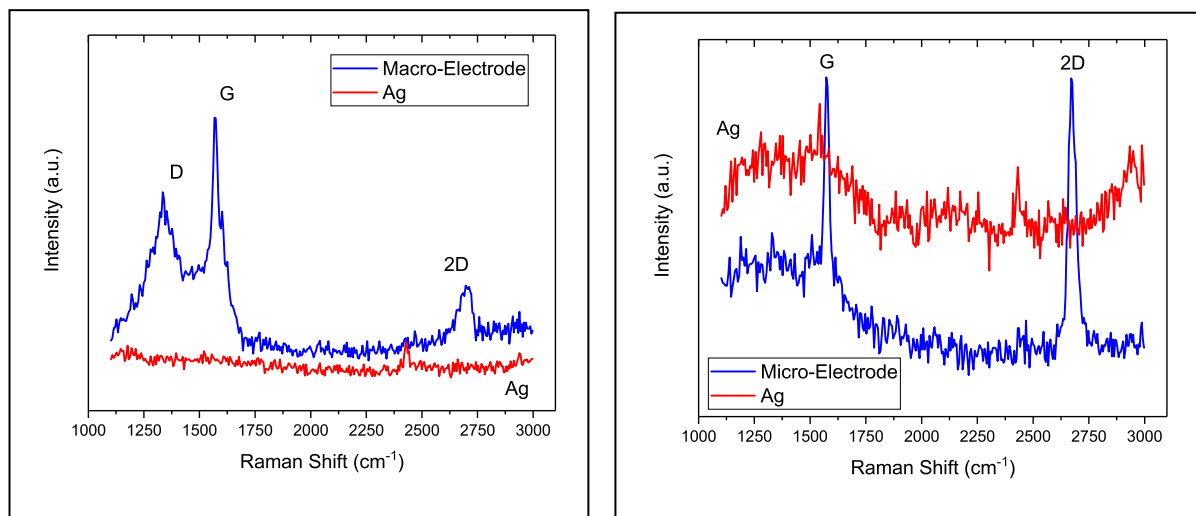
FIGURE 1. Raman spectra of bare carbon for macro- and micro-electrodes compared to Ag in locality with the working electrodes.

2D bands respectively, which correlate to known bands for carbon as reported earlier [36], [37]. The measured intensities of D, G and 2D peaks varied across different areas of the same macro or micro-electrode surfaces. In particular, the three peaks are prominent from most of the examined areas of the macro-electrode while only a few areas of the micro-electrode surface showed D peaks, which suggests the latter electrode had relatively low density of defects and disorder compared to the macro-electrode. There are several factors that can affect the Raman signal from the surface of the working electrode, such as peak position, intensity rations I(D)/I(G), I(G)/I(2D), full-width-half-maximum of the peaks, stress, doping etc. Therefore, the nature and quality of the electrode surface is found to play a significant role in influencing the sensitivity of the biosensing surface. The Raman spectrum in Figure 1 lends support to our results from the cyclic voltammetry measurements (Section C) which demonstrate that the micro-electrode is approximately an order-of-magnitude more sensitive than the macro-electrode.

B. CONTACT ANGLE ANALYSIS

The wettability of the modified sensor was investigated by studying the contact angles of water droplets on the carbon substrate. Generally, a small angle indicates a hydrophilic surface, while a large angle indicates a hydrophobic surface. The importance of investigating the wetting properties was to determine the quality of the modified surface, since the wettability has an impact on molecule immobilization [38]. In this work, contact angle data for water droplet on the unmodified carbon micro-substrate showed a hydrophilic surface (68.9°), which indicates good wettability and adhesiveness and high solid surface free energy. In contrast, the unmodified carbon macro-substrate showed a hydrophobic surface (97.9°). Further modification of the carbon macro-surface with PANHS led to lower hydrophilicity (87.8°) due

to its structural nature. The structure of PANHS includes a pyrene and amine-reactive hydrophobic region. A stable non-covalent complex can be formed between pyrene derivatives and the carbon substrate, while the NHS ester can be used to couple to amine-containing ligands such as antibodies [39]. Subsequently, functionalizing the surface with hCG antibodies and blocking with BSA decreased the angles to 63.4° and 52.5°, respectively. This reduction of contact angle values indicated an increasing wettability of the generated surface (**Figure 2**). The final developed layer revealed a hydrophilic matrix that is suitable for biomolecular immobilization and detection.

C. CHARACTERIZATION OF BARE CARBON MACRO- AND MICRO-ELECTRODES BY CYCLIC VOLTAMMETRY

Cyclic voltammetry of carbon electrodes in the presence of a redox mediator is a classic electrochemical experiment for characterizing a carbon electrode surface. **Figure 3** shows a side-by-side comparison of two electrodes, a macro-carbon-electrode and a micro-carbon-electrode, which would have been expected to give similarly shaped cyclic voltammograms when tested with a ferricyanide/ Fferrocyanide solution, but, in fact, the macro-electrode had a cyclic voltammogram that was distorted relative to the micro-electrode. The voltammograms of the macro-electrode attained its characteristic symmetrical appearance from the reversible redox reaction, but with peak separations much greater than that dictated by the Nernst equation (59 mV for single electron reactions at room temperature). This is attributed to the inherent resistance of the carbon, resulting in an internal IR voltage drop in the electrode material. This contribution is typically negligible in metallic electrodes. For the micro-electrodes, two sharp redox peaks emerged. These were closer to the expected 59mV peak separation, indicating that the resistance was significantly lowered. The reduced electrode size
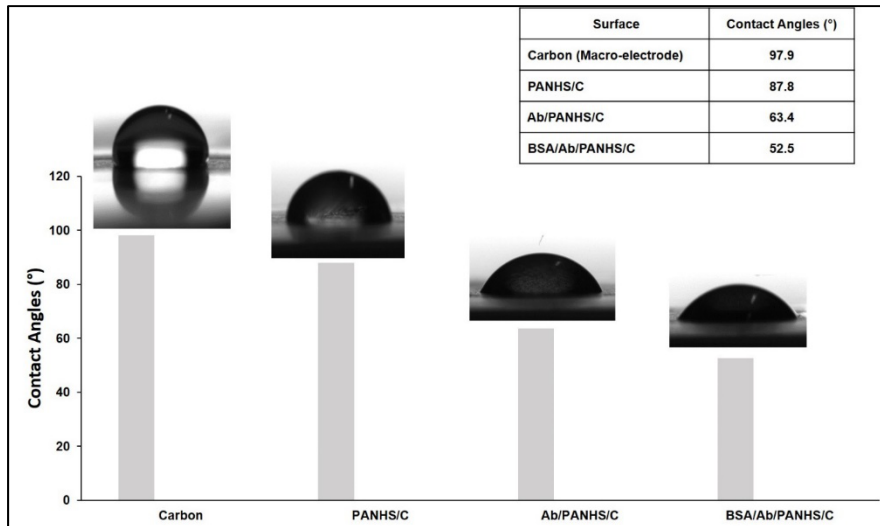
Surface	Contact Angles (°)
Carbon (Macro-electrode)	97.9
PANHS/C	87.8
Ab/PANHS/C	63.4
BSA/Ab/PANHS/C	52.5

FIGURE 2. Contact angle images of water droplets on unmodified carbon macro-electrode, PANHS-modified carbon electrode, hCG antibody / PANHS-modified carbon electrode, and BSA / Ab / PANHS-modified carbon electrode.
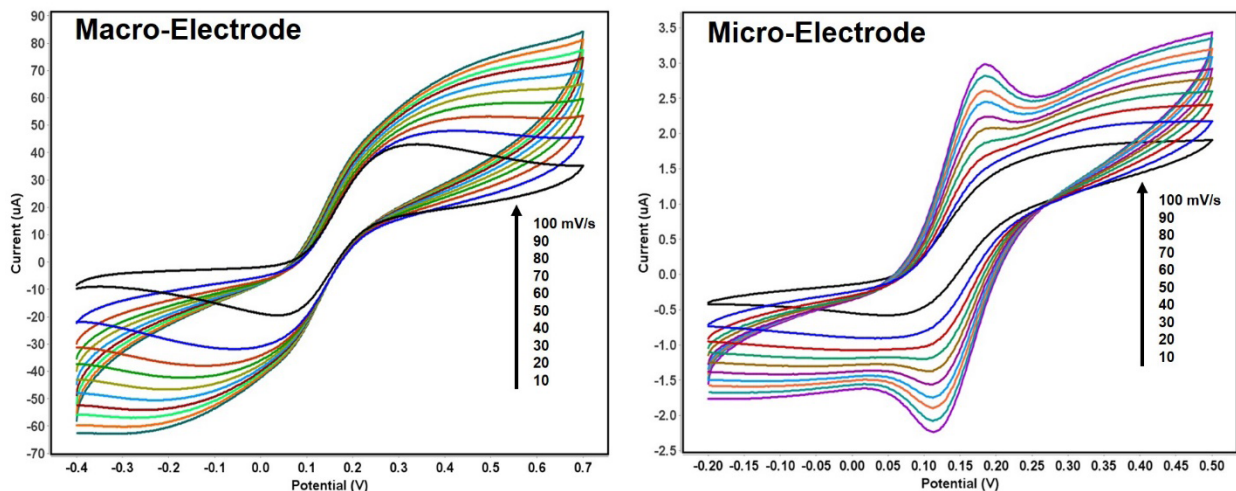

FIGURE 3. Cyclic voltammograms of the developed biosensor (C/PANHS/anti-hCG Ab/BSA) for macro- and micro-electrodes in 10 mM $[Fe(CN_6)]^{3-/4-}$ and 100 mM KCl with increasing scan rate from 10 to 100 mV/s.

lowered the resistance R, since the distance to the conductive track was shorter, in accordance with Pouillette's law:

$$R = \rho \frac{L}{A}$$

where ρ (ohm cm) is the inherent resistivity of the carbon, L (cm) is the length of the resistive material, and A (cm^2) is its cross-sectional area.

The classical Randle equivalent circuit shown in **Figure 4** can be used to explain the CV response data shown in Figure 3. We added an extra resistive element, $R_{Electrode}$, to represent the resistance of the electrode. In the case of the micro-electrode, the $R_{Electrode}$ element had a smaller value and did not distort the voltammograms, whilst in the case of the macro electrode, the $R_{Electrode}$ value was larger and started to dominate and distort the voltammograms by increasing the peak separation.
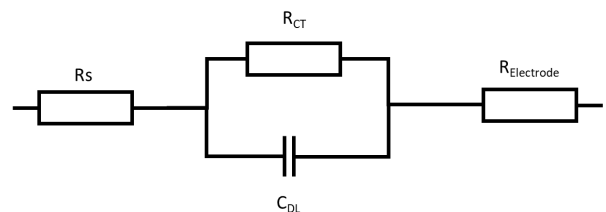

FIGURE 4. Randle Equivalent Circuit: R_S solution resistance, R_{CT} charge transfer resistance, C_{DL} double layer capacitance, $R_{Electrode}$ resistance of the electrode.

As the macro- and the micro-electrodes were from different suppliers, it is possible that the screen-printing ink was more conductive in the micro-electrode than the macro-electrode. Although the ink was from different suppliers,
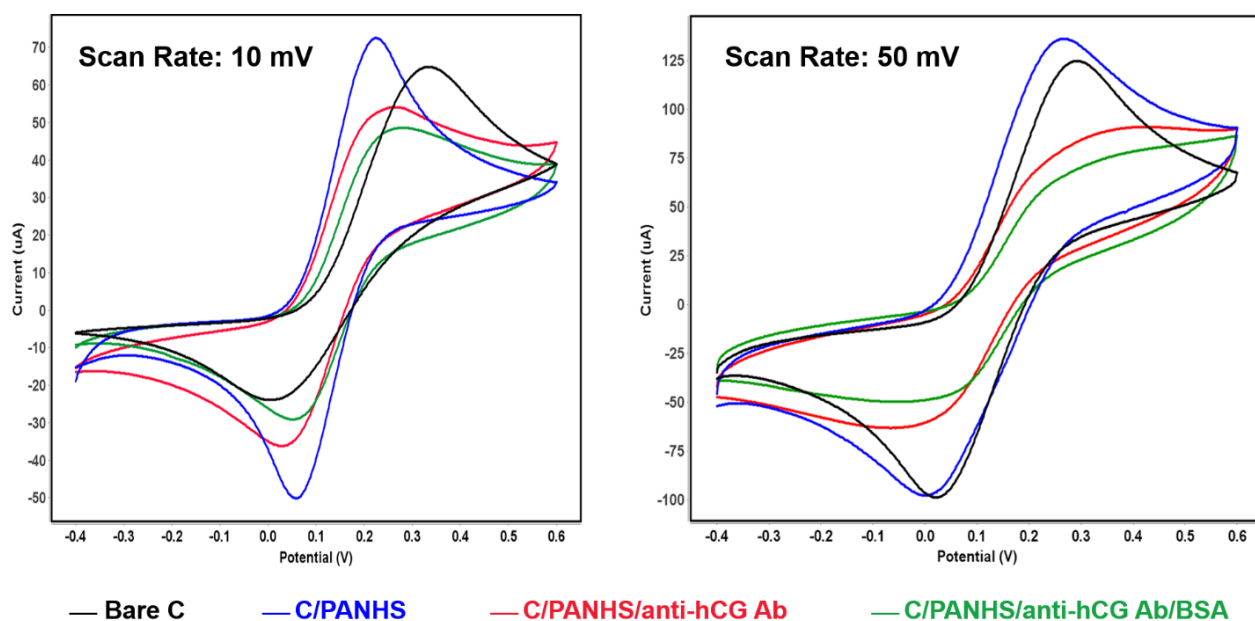
FIGURE 5. Cyclic voltammograms of macro-electrode in 10 mM [Fe(CN$_6$)]$^{3-/4-}$ and 100 mM KCl for each modification steps at scan rates 10 and 50 mV/s.

the carbon material was nominally the same with only a small variation between the ink conductivities expected ($\sim$10%). This small difference in electrode ink conductivities would only be a second-order effect, and we did not anticipate this aspect to be a major systematic effect in the sensitivity approach. For either of these screen-printed electrodes to work in this application with the necessary sensitivity, it is important that the charge transfer resistance R$_{CT}$ and the double layer capacitance, C$_{DL}$ are the dominant elements in the circuit, as the elements characterize the specific binding at the sensor surface during the assay. However, if the R$_{Electrode}$ value is too high relative to the R$_{CT}$, it will mask their contributions and therefore make the assay less sensitive. Moreover, another difference between the macro- and micro-electrodes was that the reference electrodes were Ag and Ag/AgCl, respectively. The Ag reference probably accounts for the shift of the voltammogram along the potential axis. It is, however, the same reaction occurring on the reference electrode due to Ag spontaneously forming AgCl in Cl$^-$-rich solutions [40].

D. SENSING ASSAY PRINCIPLES

Scheme 1 shows the current approach for the detection of the hCG biomarker using PANHS-modified screen-printed carbon electrodes. Carbon micro- and macro-electrodes were modified with PANHS as an intermediate layer between the antibody and the carbon surface and subsequently exposed to the solution of the anti-hCG antibody. The blocking step using BSA was performed in order to minimize any unspecific binding on the surface and was followed by the hCG antigen incubation step. The target hCG protein was captured by the immobilized hCG antibodies.

Functionalized electrodes and the detection efficiency of hCG antigen were characterized using CV and SWV measurements by monitoring Faradaic and non-Faradaic currents generated by [Fe(CN$_6$)]$^{3-/4-}$ present in the electrolyte solution. For the macro-electrode (4 mm), **Figure 5** shows the cyclic voltammograms of different components on the macro-electrode surface at scan rates of 10 and 50 mV/s. As shown in these voltammograms, typical peak-shaped current–voltage curves were obtained as well as an increase in the peak current of PANHS/C electrode compared to the bare C electrode, which can be attributed to higher electric transfer kinetics at the macro-sized working electrode surface. PANHS molecules improved the electrocatalytic behavior and increased the effective surface area, which enhanced electron transport between the mediator layer and electrode. By immobilizing the anti-hCG antibody and blocking the electrode surface, the peak current signals further reduced due to prevention of the [Fe(CN$_6$)]$^{3-/4-}$ redox system from approaching the electrode surface. Hence, it is clear that the intensity of anodic and cathodic peak currents is affected by each deposited layer on the sensor surface.

When the micro-electrode (400 μm) was used as a working electrode, the peak-shape was found to be significantly different to that of the macro-electrode (**Figure 6**). It is possible that the random distribution of the particles on the macro-electrode surface changed the electrode behavior, while in the case of micro-electrode surface, the nearest-neighbor distance minimized diffusion, which led to a higher mass transport per unit surface area. Moreover, at a lower scan rate (10 mV/s), the shape and intensity of the current–voltage curves were different compared to curves at higher scan
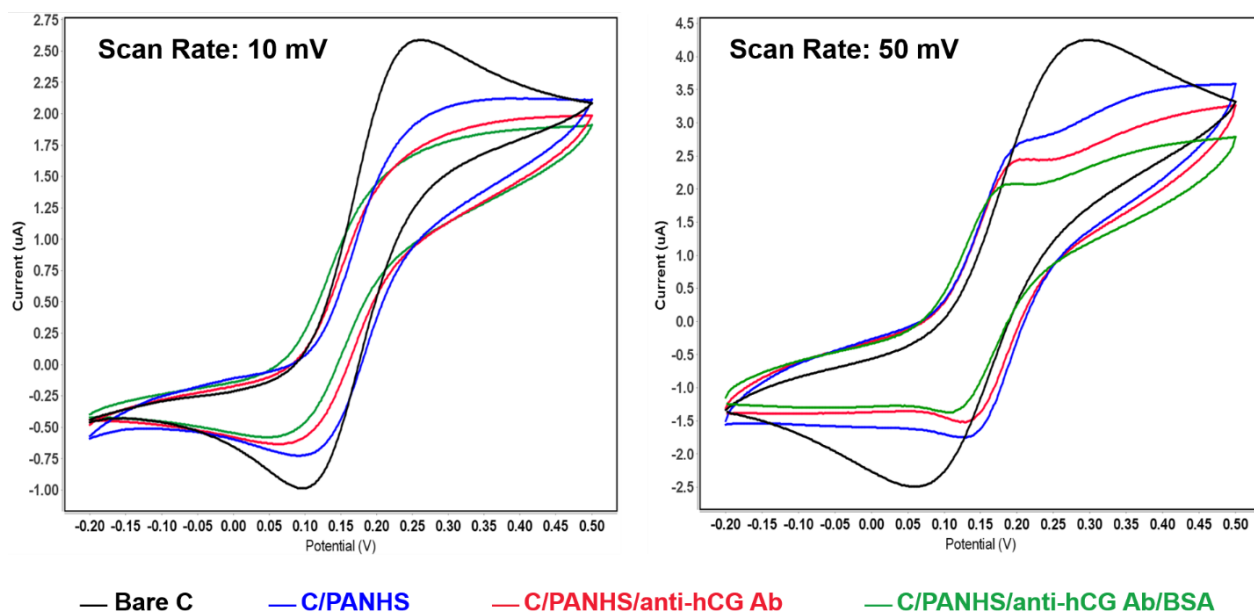
FIGURE 6. Cyclic voltammograms of micro-electrode in 10 mM $[Fe(CN_6)]^{3-/4-}$ and 100 mM KCl for each modification steps at scan rates 10 and 50 mV/s.

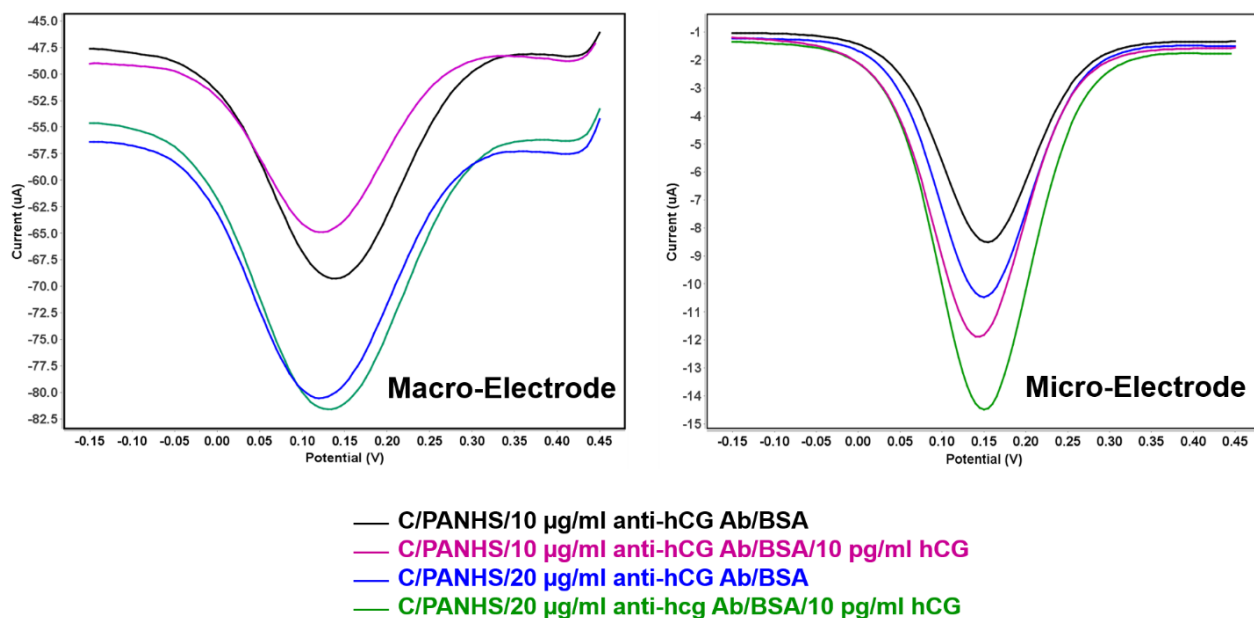**FIGURE 7.** SWV signals for optimizing of the anti-hCG antibody concentrations (10 and 20 μg/mL) on the PANHS-modified macro- and micro-electrodes and detection of 10 pg/mL hCG protein in 10 mM $[Fe(CN_6)]^{3-/4-}$ and 100 mM KCl. Potential step: 5 mV; amplitude: 25 mV; frequency: 15 Hz.

rates (50 mV/s). However, after modifying the carbon electrode with PANHS molecules, in contrast to the macro-electrode, the value of the peak current decreased, which indicated formation of an insulation layer that hinders the electron transfer between the linker layer and the electrode. Similar to the macro-electrode, the current signals decreased with the stepwise addition of the antibodies and

BSA molecules. The subsequent reduction of CV signals after addition of these biomolecules indicates formation of a functional biosensor and the effects of different sized working electrodes. The results of the CV studies conducted on the BSA/anti-hCG antibody/PANHS/CE biosensor obtained as a function of scan rates from 10 to 10 0mV/s are shown in Figure 3 for macro- and micro-electrodes.
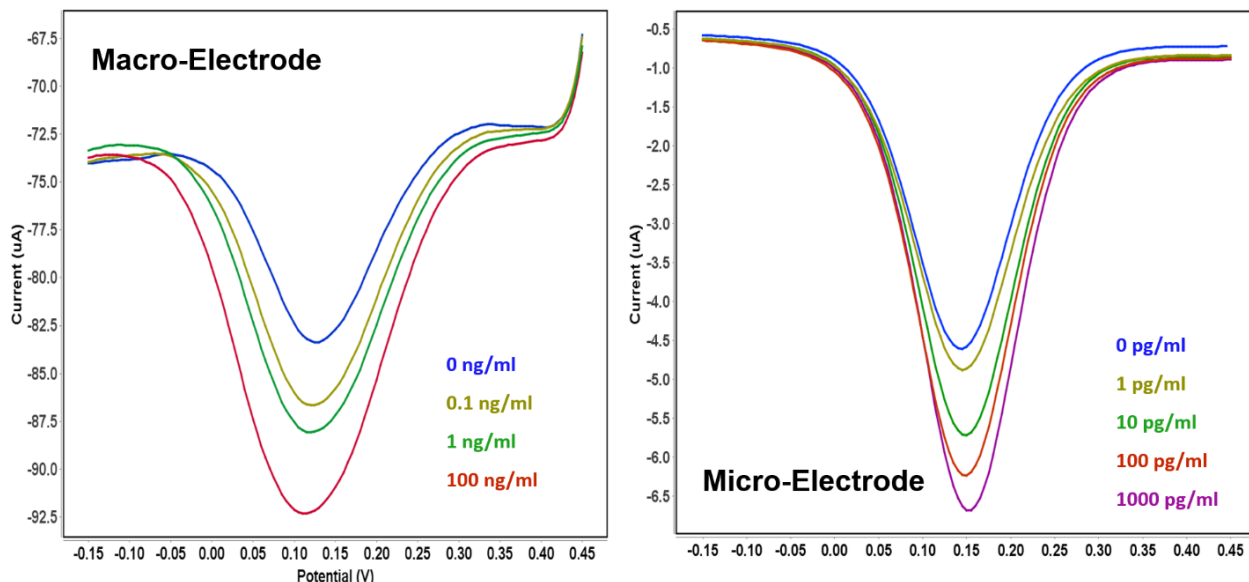
FIGURE 8. Change of SWV signals at the developed immunesensor of macro- and micro-electrodes after incubation with hCG protein at different concentrations.

TABLE 1. Comparison of reported biosensors for hCG detection.

Electrode Architecture	Electrochemical Method	LoD	Reference
Anti-hCG/ PANHS/ graphene	field-effect transistor (FET)	1 pg/mL	17
AgNP/ ionic liquid- chitosan- graphene (Gr-IL-Chit)/ CE	Differential Pulse Voltammetry (DPV)	0.0066 mIU/ml	32
HRP-anti-HCG-HCG/ titania sol–gel film	DPV	1.4 mIU/ml	33
Anti-hCG/ nano-Au/ Methyleneblue (MB)/ CE	CV	3 pg/mL	43
Anti hCG/ nanoporous gold foils (NPG)/ graphene sheets (Gs) /CE	Amperometric	0.034 ng/mL	44
Anti-hCG/ PANHS/ micro CE	SWV	1 pg/mL	This study

E. OPTIMIZATION OF THE SENSING SYSTEM

Finding the optimal concentration of the immobilized recognition biomolecules (e.g., antibodies) on sensor surface significantly improved the selectivity and sensitivity of the sensing system. **Figure 7** shows changes in the SWV current in response to the detection of 10 pg/mL of the hCG antigen with two different concentrations of the anti-hCG antibody (10 and 20 μg/mL). In the case of the micro-electrode, in response to 10 pg/mL of the hCG antigen, both concentrations of the immobilized hCG antibody (10 and 20 μg/mL) effectively reduced the SWV current ($\sim$40%) in comparison to the PANHS layer without antibodies. In contrast, when the macro-electrode was tested, neither of these two antibody concentrations gave consistent antigen detection by the macro-electrode. However, 20 μg/mL was selected as the optimal hCG antibody concentration, which was high

enough to recognize 10 pg/mL of the hCG antigen. Although, 10 μg/mL of the antibody exhibited good sensitivity to hCG antigen capture, this concentration was excluded. A low antibody concentration may not be sufficient to target the antigen, which further reduces the sensitivity of a designed sensor. In contrast, a high antibody concentration increases the antibody layer density, which may generate high steric barrier that prohibits $[Fe(CN_6)]^{3-/4-}$ ions from moving onto the electrode surface.

F. CHARACTERIZATION OF SENSITIVITY OF THE MODIFIED ELECTRODES

To investigate the sensitivity and analytical performance of the developed macro- and micro-biosensors, the hCG biomarker was used at different concentrations in PBS, and electrochemical response studies were performed in
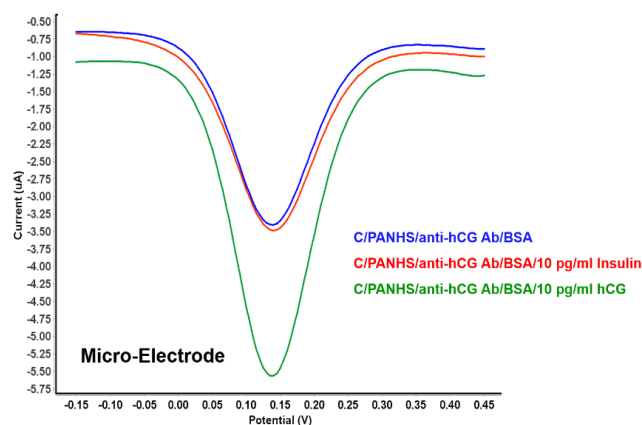
FIGURE 9. SWV signals obtained at the modified micro-electrode (C/PANHS/anti-hCG Ab/BSA) with hCG protein and insulin (as a negative control).

$[Fe(CN_6)]^{3-/4-}$ using the SWV technique with an amplification of 25 mV and a frequency of 15 Hz. For the macro-electrode (**Figures 8**), during the SWV measurements, the peak current reduced with increasing hCG concentrations, which is attributed to formation of an antigen–antibody complex onto the developed electrode. The limit of detection was approximately 0.1ng/mL, and higher hCG concentrations (>100 ng/mL) caused surface saturation (data not shown).

Typical voltammograms for the performance of the micro-electrode in detecting hCG at concentrations of 1, 10, 100, and 1000 pg/mL are shown in Figure 8. The micro-electrode showed higher sensitivity compared with the macro-electrodes. It was able to detect hCG at a concentration level as low as 1 pg/mL, and sensor surface became saturated at a concentration higher than 1000 pg/mL. The obtained results confirmed the good sensitivity of the fabricated bioelectrodes. Moreover, as shown above using Raman spectroscopy, the micro-electrode has better structural properties which also indicates potential for enhanced sensitivity of this type of sensing surface. **Table 1** shows the limit of detection for previously reported biosensors to detect hCG using various electrochemical methods.

To confirm the selectivity for the hCG protein, the modified micro-electrode sensor was tested by incubation with 10 pg/mL insulin, and its response was compared to hCG at the same concentration (**Figure 9**). The control experiment showed no significant changes after the addition of insulin to the developed sensor, while a significant response was recorded with hCG due to the specific interaction between the antibody and antigen.

IV. CONCLUSION

In this study, the physical size of the working electrode was demonstrated to have a direct impact on the electrochemical response and sensitivity of fabricated biosensors using macro- and micro-electrodes. The results of CV and SWV measurements conducted on the developed BSA/anti-hCG antibody/PANHS/SPCE showed the generation of a

simple, low-cost, and label-free electrochemical biosensor with good selectivity and sensitivity for the hCG protein. The macro-electrode showed typical voltammogram peaks for the fabricated sensor and acceptable detection limit (100 pg/mL), whereas the micro-electrodes showed higher sensitivity (1 pg/mL), which may be attributed to better structural properties due to the nearest-neighbor distance, as confirmed by Raman spectroscopy, and the more favorable electrochemical properties of the micro-electrode relative to the macro-electrode due to the lowered electronic resistance, as evidenced by CV characterization. Future work will aim to modify the proposed sensors by using different carbon materials, such as graphene, and two-dimensional materials [41] to investigate the electrochemical behaviors of different matrices based on the surface area, to enhance the sensitivity, and to target different sample types as well as impedance spectroscopy detection techniques [42]. Indeed, the principles of the presented assay can be exploited to fabricate a variety of diagnostic sensors by using different antibodies or aptamers to recognize a wide range of biomarkers.

REFERENCES

[1] F. Darain, K. L. Gan, and S. C. Tjin, "Antibody immobilization on to polystyrene substrate—On-chip immunoassay for horse IgG based on fluorescence," *Biomed. Microdevices*, vol. 11, no. 3, pp. 653–661, 2009.

[2] S. Damiati, S. Küpcü, M. Peacock, C. Eilenberger, M. Zamzami, I. Qadri, H. Choudhry, U. B. Sleytr, and B. Schuster, "Acoustic and hybrid 3D-printed electrochemical biosensors for the real-time immunodetection of liver cancer cells (HepG2)," *Biosensors Bioelectron.*, vol. 94, pp. 500–506, Aug. 2017.

[3] S. Damiati, M. Peacock, R. Mhanna, S. Søpstad, U. B. Sleytr, and B. Schuster, "Bioinspired detection sensor based on functional nanostructures of S-proteins to target the folate receptors in breast cancer cells," *Sens. Actuators B, Chem.*, vol. 267, pp. 224–230, Aug. 2018.

[4] F. Islam, M. H. Haque, S. Yadav, M. N. Islam, V. Gopalan, N.-T. Nguyen, A. K. Lam, and M. J. A. Shiddiky, "An electrochemical method for sensitive and rapid detection of FAM134B protein in colon cancer samples," *Sci. Rep.*, vol. 2017, Mar. 2017, Art. no. 133.

[5] M. J. A. Shiddiky, H. Park, and Y.-B. Shim, "Direct analysis of trace phenolics with a microchip: In-channel sample preconcentration, separation, and electrochemical detection," *Anal. Chem.*, vol. 78, no. 19, pp. 6809–6817, 2006.

[6] J. Lin and H. Ju, "Electrochemical and chemiluminescent immunosensors for tumor markers," *Biosensors Bioelectron.* vol. 20, no. 8, pp. 1461–1470, 2005.

[7] S. Damiati, M. Peacock, S. Leonhardt, L. Damiati, M. A. Baghdadi, H. Becker, R. Kodzius, and B. Schuster, "Embedded disposable functionalized electrochemical biosensor with a 3D-printed flow cell for detection of hepatic oval cells (HOCs)," *Genes*, vol. 9, no. 2, p. 89, 2018.

[8] A. V. Nabok, A. Tsargorodskaya, A. K. Hassan, and N. F. Starodub, "Total internal reflection ellipsometry and SPR detection of low molecular weight environmental toxins," *Appl. Surf. Sci.*, vol. 246, no. 4, pp. 381–386, 2005.

[9] L. Yu, Y. Zhang, C. Hu, H. Wu, Y. Yang, C. Huang, and N. Jia, "Highly sensitive electrochemical impedance spectroscopy immunosensor for the detection of AFB_1 in olive oil," *Food Chem.*, vol. 176, pp. 22–26, Jun. 2015.

[10] M. Badea, L. Floroian, P. Restani, and M. Moga, "Simple surface functionalization strategy for immunosensing detection of aflatoxin B1," *Int. J. Electrochem. Sci.*, vol. 11, pp. 6719–6734, Jul. 2016.

[11] B. R. Scharifker, J. Bockris, B. E. Conway, and R. E. White, Eds., *Modern Aspects of Electrochemistry*, no. 22. New York, NY, USA: Plenum, 1992, p. 467.

[12] K. B. Oldham, "All steady-state microelectrodes have the same 'iR drop,'" *J. Electroanal. Chem. Interfacial Electrochem.*, vol. 237, no. 2, pp. 303–307, 1987.

[13] S. Bruckenstein, "Ohmic potential drop at electrodes exhibiting steady-state diffusional currents," *Anal. Chem.*, vol. 59, no. 17, pp. 2098–2101, 1987.

[14] A. M. Bond, D. Luscombe, K. B. Oldham, and C. G. Zoski, "A comparison of the chronoamperometric response at inlaid and recessed disc microelectrodes," *J. Electroanal. Chem. Interfacial Electrochem.*, vol. 249, nos. 1–2, pp. 1–14, 1988.

[15] H.-P. Nirmaier and G. Henze, "Characteristic behavior of macro-, semimicro- and microelectrodes in voltammetric and chronoamperometric measurements," *Electroanalysis*, vol. 9, no. 8, pp. 619–624, 1997.

[16] J. P. Metters and C. E. Banks, "Screen printed electrodes open new vistas in sensing: Application to medical diagnosis," in *Applications of Electrochemistry in Medicine*, vol. 56, M. Schlesinger, Ed. New York, NY, USA: Springer, 2013, pp. 83–120.

[17] C. Haslam, S. Damiati, T. Whitley, P. Davey, E. Ifeachor, and S. A. Awan, "Label-free sensors based on graphene field-effect transistors for the detection of human chorionic gonadotropin cancer risk biomarker," *Diagnostics*, vol. 8, no. 1, p. 5, 2018.

[18] K. Islam, S. Damiati, J. Sethi, A. Suhail, and G. Pan, "Development of a label-free immunosensor for clusterin detection as an alzheimer's biomarker," *Sensors*, vol. 18, no. 1, p. 308, 2018.

[19] J. S. Y. Chia, M. T. T. Tan, P. S. Khiew, J. K. Chin, and C. W. Siong, "A bio-electrochemical sensing platform for glucose based on irreversible, non-covalent pi–pi functionalization of graphene produced via a novel, green synthesis method," *Sens. Actuators B, Chem.*, vol. 210, pp. 558–565, Apr. 2015.

[20] H.-P. Peng, Y. Hu, P. Liu, Y.-N. Deng, P. Wang, W. Chen, A.-L. Liu, Y.-Z. Chen, and X.-H. Lin, "Label-free electrochemical DNA biosensor for rapid detection of mutidrug resistance gene based on Au nanoparticles/toluidine blue–graphene oxide nanocomposites," *Sens. Actuators B, Chem.*, vol. 207, pp. 269–276, Feb. 2015.

[21] A. Benvidi, M. D. Tezerjani, S. Jahanbani, M. M. Ardakani, and S. M. Moshtaghioun, "Comparison of impedimetric detection of DNA hybridization on the various biosensors based on modified glassy carbon electrodes with PANHS and nanomaterials of RGO and MWCNTs," *Talanta*, vol. 147, pp. 621–627, Jan. 2016.

[22] R. J. Chen, Y. Zhang, D. Wang, and H. Dai, "Noncovalent sidewall functionalization of single-walled carbon nanotubes for protein immobilization," *J. Amer. Chem. Soc.*, vol. 123, no. 16, pp. 3838–3839, 2001.

[23] R. E. Canfield, J. F. O'Connor, S. Birken, A. Krichevsky, and A. J. Wilcox, "Development of an assay for a biomarker of pregnancy and early fetal loss," *Environ. Health Perspect.*, vol. 74, pp. 57–66, Oct. 1987.

[24] L. A. Cole, "HCG variants, the growth factors which drive human malignancies," *Amer. J. Cancer Res.*, vol. 2, no. 1, pp. 22–35, 2012.

[25] M. Szturmowicz, J. Slodkowska, J. Zych, P. Rudzinski, A. Sakowicz, and E. Rowinska-Zakrzewska, "Frequency and clinical significance of β-subunit human chorionic gonadotropin expression in non-small cell lung cancer patients," *Tumor Biol.*, vol. 20, no. 2, pp. 99–104, 1999.

[26] B. Rau, C. Below, W. Haensch, W. Liebrich, S. C. von, and P. M. Schlag, "Significance of serum beta-hCG as a tumor marker for stomach carcinoma," *Langenbecks Archiv Chirurgie*, vol. 380, no. 6, pp. 359–364, 1995.

[27] J. Louhimo, H. Alfthan, U.-H. Stenman, and C. Haglund, "Serum HCGβ and CA 72-4 are stronger prognostic factors than CEA, CA 19-9 and CA 242 in pancreatic cancer," *Oncology*, vol. 66, no. 2, pp. 126–131, 2004.

[28] M. Kinugasa, R. Nishimura, T. Koizumi, K. Morisue, T. Higashida, T. Natazuka, T. Nakagawa, T. Isobe, S. Baba, and K. Hasegawa, "Combination assay of urinary beta-core fragment of human chorionic gonadotropin with serum tumor markers in gynecologic cancers," *Jpn. J. Cancer Res.*, vol. 86, no. 8, pp. 783–789, 1995.

[29] P. L. Triozzi and V. C. Stevens, "Human chorionic gonadotropin as a target for cancer vaccines," *Oncol. Rep.*, vol. 6, no. 1, pp. 7–24, 1999.

[30] M. Roushani, A. Valipour, and M. Valipour, "Layer-by-layer assembly of gold nanoparticles and cysteamine on gold electrode for immunosensing of human chorionic gonadotropin at picogram levels," *Mater. Sci. Eng., C*, vol. 61, pp. 344–350, Apr. 2016.

[31] K. Charoenkitamorn, P. T. Tue, K. Kawai, O. Chailapakul, and Y. Takamura, "Electrochemical immunoassay using open circuit potential detection labeled by platinum nanoparticles," *Sensors*, vol. 18, no. 2, p. 444, 2018.

[32] M. Roushani and A. Valipour, "Voltammetric immunosensor for human chorionic gonadotropin using a glassy carbon electrode modified with silver nanoparticles and a nanocomposite composed of graphene, chitosan and ionic liquid, and using riboflavin as a redox probe," *Microchimica Acta*, vol. 183, no. 2, pp. 845–853, 2016.

[33] J. Chen, F. Yan, Z. Dai, and H. Ju, "Reagentless amperometric immunosensor for human chorionic gonadotrophin based on direct electrochemistry of horseradish peroxidase," *Biosensors Bioelectron.*, vol. 21, no. 2, pp. 330–336, 2005.

[34] S. Teixeira, R. S. Conlan, O. J. Guy, and M. G. F. Sales, "Novel single-wall carbon nanotube screen-printed electrode as an immunosensor for human chorionic gonadotropin," *Electrochimica Acta*, vol. 136, pp. 323–329, Aug. 2014.

[35] Z. Chen, S. M. Tabakman, A. P. Goodwin, M. G. Kattah, D. Daranciang, X. Wang, G. Zhang, X. Li, Z. Liu, P. J. Utz, K. Jiang, S. Fan, and H. Dai, "Protein microarrays with carbon nanotubes as multicolor Raman labels," *Nature Biotechnol.*, vol. 26, pp. 1285–1292, Oct. 2008.

[36] J.-G. Li, C.-Y. Tsai, and S.-W. Kuo, "Fabrication and characterization of inorganic silver and palladium nanostructures within hexagonal cylindrical channels of mesoporous carbon," *Polymers*, vol. 6, no. 6, pp. 1794–1809, 2014.

[37] M. Saravanan, M. Ganesan, and S. Ambalavanan, "An *in situ* generated carbon as integrated conductive additive for hierarchical negative plate of lead-acid battery," *J. Power Sources*, vol. 251, pp. 20–29, Apr. 2014.

[38] B. Derkus, K. C. Emregul, and E. Emregu, "Evaluation of protein immobilization capacity on various carbon nanotube embedded hydrogel biomaterials," *Mater. Sci. Eng., C*, vol. 56, pp. 132–140, Nov. 2015.

[39] G. T. Hermanson, "Buckyballs, fullerenes, and carbon nanotubes," in *Bioconjugate Techniques*. New York, NY, USA: Academic, 2013, pp. 741–755. doi: 10.1016/B978-0-12-382239-0.00026-1.

[40] S. Søpstad, E. A. Johannessen, F. Seland, and K. Imenes, "Long-term stability of screen-printed pseudo-reference electrodes for electrochemical biosensors," *Electrochimica Acta*, vol. 287, pp. 29–36, Oct. 2018.

[41] S. A. Awan, A. Lombardo, A. Colli, G. Privitera, T. S. Kulmala, J. M. Kivioja, M. Koshino, and A. C. Ferrari, "Transport conductivity of graphene at RF and microwave frequencies," *2D Mater.*, vol. 3, no. 1, pp. 015010-1–015010-11, 2016.

[42] S. A. Awan, G. Pan, L. M. Al Taan, B. Li, and N. Jamil, "Radio-frequency transport Electromagnetic Properties of chemical vapour deposition graphene from direct current to 110 MHz," *IET Circuits, Devices Syst.*, vol. 9, no. 1, pp. 46–51, Jan. 2015.

[43] R. Chai, R. Yuan, Y. Chai, C. Ou, S. Cao, and X. Li, "Amperometric immunosensors based on layer-by-layer assembly of gold nanoparticles and methylene blue on thiourea modified glassy carbon electrode for determination of human chorionic gonadotrophin," *Talanta*, vol. 74, no. 5, pp. 1330–1336, 2008.

[44] R. Li, D. Wu, H. Li, C. Xu, H. Wang, Y. Zhao, Y. Cai, Q. Wei, and B. Du, "Label-free amperometric immunosensor for the detection of human serum chorionic gonadotropin based on nanoporous gold and graphene," *Anal. Biochem.*, vol. 414, no. 2, pp. 196–201, 2011.

SAMAR DAMIATI received the Ph.D. degree from the Institute of Synthetic Bioarchitectures, Department of Nanobiotechnology, University of Natural Resources and Life Sciences (BOKU), Vienna, Austria, in 2013. She is currently an Associate Professor with the Biochemistry Department, King Abdulaziz University (KAU), Jeddah, Saudi Arabia. Her current research interests include development of synthetic bioarchitectures that mimic the biological ones, fabrication of acoustic and electrochemical biosensors for the detection of various biomarkers, and designing and testing microfluidic devices for several applications.

CARRIE HASLAM received the degree (Hons.) in bioveterinary science. She is currently pursuing the Ph.D. degree with the University of Plymouth. She is working on developing encapsulated chemical vapour deposition (CVD) graphene field-effect (GFET) immunosensors for the sensitive detection of a prominent candidate biomarker of Alzheimer's Disease (AD), Clusterin (CLU). Her work has been published within numerous academic journals, as well as presented at both national and international conferences.

SINDRE SØPSTAD received the B.Eng. degree in electronics engineering and the M.Sc. degree in microsystems technology from the University of South-Eastern Norway (USN), in 2013 and 2015, respectively, where he is currently pursuing the Ph.D. degree in applied microsystems, centered around the work presented in this paper. He has been involved in part-time with biosensor development company Zimmer and Peacock, Horten, Norway, since 2012. His research interests include span electrochemical sensor development, electronic front-end design, and automated data analysis.

MARTIN PEACOCK is an Industrial Bioelectrochemist with over 20 years of biosensor experience, having industrial roles from Abbott Diabetes to GSK and solving technical challenges from continuous glucose monitoring to RNA analysis. He has set-up biosensor focused companies across the globe from Silicon Valley California to Oslo Norway.

TOBY WHITLEY received the PhD degree in electronic and communications engineering from Bristol University, where he pursued the Ph.D. degree in high speed wireless communications, focusing on Handover and Quality of Service. He has held a number of teaching and research positions first at Bristol and then the University of Bath, working on sensors operating in the ELF band up into the GHz range. He is currently the Associate Head of the Electronics and Robotics subjects with Plymouth University.

PAUL DAVEY is currently an Associate Professor (Senior Lecturer) in electronics and embedded systems with the School of Computing, Electronics and Mathematics. His research interests include embedded system design, digital signal processing and coding for magnetic and optical storage systems, information sensing and security, renewable energy, and graphene sensors and nanotechnology. He has been involved in number of successful KTPs, industrially funded research and is currently a Co-Investigator on the EU H2020 Marie-Curie ETN with funding totalling £3.2M. He has also been the Director of Studies for three Ph.D. students and Co-Supervisor for nine Ph.D. students to completion.

SHAKIL A. AWAN He was a Lecturer and the Director of Studies with the Newnham College, University of Cambridge, and a Senior Research Scientist with the National Physical Laboratory. He is currently a Lecturer with the School of Computing, Electronics and Mathematics, University of Plymouth, U.K. He has extensive experience in precision measurements in solid state physics/superconductivity, ac & dc quantum hall effect, MEMS, and Impedance Standards as well as MRI and for the last 10 years in graphene electron transport physicsand high-speed electronics and sensors for Alzheimer's biomarker detection.

• • •